

## Near-Infrared Fluorescence Imaging of Liver Metastases in Rats using Indocyanine Green

Joost R. van der Vorst, M.D.,\* Merlijn Hutteman, M.Sc.,\* J. Sven D. Mieog, M.D.,\* Karien E. de Rooij, Ph.D.,†,§  
Eric L. Kaijzel, Ph.D.,† Clemens W. G. M. Löwik, Ph.D.,† Hein Putter, Ph.D.,‡ Peter J. K. Kuppen, Ph.D.,\*  
John V. Frangioni, M.D., Ph.D.,||,¶ Cornelis J. H. van de Velde, M.D., Ph.D.,\*  
and Alexander L. Vahrmeijer, M.D., Ph.D.\*<sup>1</sup>

\*Department of Surgery, Leiden University Medical Center, Leiden, The Netherlands; †Department of Endocrinology, Leiden University Medical Center, Leiden, The Netherlands; ‡Department of Medical Statistics, Leiden University Medical Center, Leiden, The Netherlands; §Perucros B.V., Leiden, The Netherlands; ||Department of Medicine, Beth Israel Deaconess Medical Center, Boston, Massachusetts; and ¶Department of Radiology, Beth Israel Deaconess Medical Center, Boston, Massachusetts

Originally submitted October 29, 2010; accepted for publication January 4, 2011

**Background.** Near-infrared (NIR) fluorescence imaging using indocyanine green (ICG) is a promising technique to obtain real-time assessment of the extent and number of colorectal liver metastases during surgery. The current study aims to optimize dosage and timing of ICG administration.

**Materials and Methods.** Liver tumors were induced in 18 male WAG/Rij rats by subcapsular inoculation of CC531 rat colorectal cancer cells into three distinct liver lobes. Rats were divided in two groups: imaging after 24 and 48 h or 72 and 96 h after intravenous ICG administration. In each time group, rats were allocated to three dose groups: 0.04, 0.08, or 0.16 mg ICG. Intraoperative imaging and *ex vivo* measurements were performed using the Mini-FLARE imaging system and confirmed by fluorescence microscopy. Fluorescence intensity was quantified using the Mini-FLARE software and the difference between tumor signal and liver signal (tumor-to-liver ratio; TLR) was calculated.

**Results.** In all 18 rats, all colorectal liver metastases ( $n = 34$ ), some as small as 1.2 mm, were identified using ICG and the Mini-FLARE imaging system. Average tumor-to-liver ratio (TLR) over all groups was  $3.0 \pm 1.2$ . TLR was significantly higher in the 72 h time group compared with other time points. ICG dose did not significantly influence TLR, but a trend was found favoring the 0.08 mg dose group. Fluorescence microscopy demonstrated a clear fluorescent rim around the tumor.

<sup>1</sup> To whom correspondence and reprint requests should be addressed at Department of Surgery, Leiden University Medical Center, Albinusdreef 2, 2300 RC Leiden, The Netherlands. E-mail: [a.l.vahrmeijer@lumc.nl](mailto:a.l.vahrmeijer@lumc.nl).

**Conclusions.** This study demonstrates that colorectal cancer liver metastases can be clearly identified during surgery using ICG and the Mini-FLARE imaging system, with optimal timing of 72 h post-injection and an optimal dose of 0.08 mg (0.25 mg/kg) ICG. NIR fluorescence imaging has the potential to improve intraoperative detection of micrometastases and, thus, the completeness of resection.

© 2012 Elsevier Inc. Open access under the [Elsevier OA license](http://creativecommons.org/licenses/by/3.0/).

**Key Words:** near-infrared fluorescence imaging; image-guided surgery; liver surgery; colorectal cancer liver metastases; indocyanine green.

### INTRODUCTION

With a worldwide annual incidence of approximately 1 million cases and an annual mortality of over 500,000 cases, colorectal cancer is the second cause of cancer death worldwide [1]. The survival of patients with colorectal carcinoma is mostly determined by the occurrence of distant metastases. Approximately 30% of patients with CRC eventually develop liver metastases [2, 3]. When metastases are confined to the liver and are resectable, surgical resection can offer a 5-y survival rate of 35% to 40% [3, 4]. Despite improved surgical techniques, preoperative imaging modalities, and improved chemotherapy regimens, intrahepatic recurrence rates vary from 11% to 26% [5–8]. This is possibly due to an inadequate assessment of the extent of disease before and during liver surgery. Currently, the most frequently used imaging modalities to make this assessment are computed tomography (CT) and intraoperative ultrasonography (IOUS). However, even

with the combined use of these modalities, 6% to 20% of liver metastases cannot be identified [9–11]. In particular, the detection of small (<5 mm) liver metastases and superficially located liver metastases appears to be difficult [11]. New imaging modalities are necessary to facilitate a more complete assessment of the extent of disease.

Near-infrared (NIR) fluorescence imaging is a promising technique to intraoperatively assess the extent of colorectal liver metastases. Recently, Ishizawa and colleagues [12] have shown that primary hepatocellular carcinoma and colorectal liver metastases could be identified using NIR fluorescence imaging and the NIR fluorescent agent indocyanine green (ICG). Colorectal liver metastases could be identified by a fluorescent rim around the metastases. They hypothesized that this distinct fluorescent pattern is probably based on biliary excretion disorders in the surrounding normal liver tissue that is compressed by expanding pressure of the tumor. In their study of 49 patients, a fixed dose of 0.5 mg/kg ICG was administered preoperatively as part of a routine ICG clearance test, which is commonly used in Asia to plan the safe extent of hepatectomy. The interval between administration of ICG and surgery varied between 1 to 7 d. Consequently, the optimal dose of ICG and time of administration before surgery remain unclear.

The goal of our study was to determine the optimal ICG dose and administration time before surgery, using a syngeneic rat model of colorectal cancer metastases in conjunction with the Mini-FLARE image-guided surgery system.

## MATERIALS AND METHODS

### Animal Model

The colorectal cancer rat CC531 cell line was used for this study. The cell line and the induction of liver metastases have been described previously [13]. In short, cells were cultured in RPMI 1640 supplemented with 2 mM L-glutamine (Gibco, Invitrogen Ltd, Carlsbad, CA), 10% heat-inactivated fetal calf serum, 100 U/mL penicillin, and 0.1 mg/mL streptomycin sulfate. In order to induce liver metastases, CC531-syngeneic male WAG/Rij rats (Harlan, Horst, The Netherlands) weighing approximately 300–350 g underwent median laparotomy and the liver was mobilized and exposed. Subsequently, 125,000 CC531 cells (in 50  $\mu$ L PBS) were subcapsularly inoculated into the left and right main liver lobes and the right accessory liver lobe [13]. Four weeks after inoculation, metastases ranging from 1.2 to 13.4 mm in size had originated in the liver.

The weight of the animals was followed throughout the experiment to monitor their general health state. Throughout tumor inoculation, injection of ICG and imaging, the animals were anesthetized with 5% isoflurane for induction and 2% isoflurane for maintenance in oxygen with a flow of 0.8 L/min. During anesthesia, the respiration rate was constantly monitored. For postoperative analgesia, the analgesic buprenorphine (0.1 mg/kg) was used. The Animal Welfare Committee of the Leiden University Medical Center approved the experiments. All animals were housed in the animal facility of the Leiden

University Medical Center. Pellet food and fresh tap water were provided *ad libitum*.

### NIR Fluorescent Contrast Agent

The clinically available NIR fluorescent contrast agent ICG (Pulsion Medical Systems, Munich, Germany) was used. Three ICG dose groups were tested: 0.04, 0.08, and 0.16 mg. Before injection, ICG powder was resuspended in 200  $\mu$ L sterile water.

### Intraoperative NIR Fluorescence Imaging System

Imaging of liver metastases was performed using the Mini-FLARE imaging system [14], which is a miniaturized version of the FLARE imaging system [15]. Briefly, the system consists of two wavelength-isolated light sources: a “white” light source, generating 26,600 l  $\times$  of 400–650 nm light and a “near infrared” light source, generating 7.7 mW/cm<sup>2</sup> of 760 nm light. Color video and NIR fluorescence images are simultaneously acquired and displayed in real-time using custom optics and software that separate the color video and NIR fluorescence images. A pseudo-colored (lime green) merged image of the color video and NIR fluorescence images is also displayed. The imaging head is attached to a flexible gooseneck arm, which permits positioning of the imaging head virtually anywhere over the surgical field, and at extreme angles.

### Experimental Design

In a time-dependent and dose-dependent experiment, NIR fluorescence imaging was performed in 18 tumor-bearing rats. To minimize surgery-related trauma and distress, rats were divided in two groups: imaging after 24 and 48 h, and imaging after 72 and 96 h of ICG administration. In each time group, rats were allocated to three dose groups of 0.04, 0.08, or 0.16 mg ICG, which was administered intravenously *via* the penile vein. Each dose group contained three rats. ICG dose levels were chosen based on clinically relevant doses using human body weight and correspond to doses of 10, 20, and 40 mg of ICG. The imaging time-points were chosen based on Ishizawa *et al.* [12] who reported NIR fluorescence imaging is preferably performed at least 24 h after ICG administration. Furthermore, for clinical translation, these time-points must be logistically acceptable to use in a clinical setting. For intraoperative imaging, the liver and other intra-abdominal organs were exposed after median laparotomy. After the first intraoperative imaging session (24 or 72 h after ICG administration), the abdomen was closed in two layers and the animal was imaged again 24 h later. At all time-points, tumor fluorescence and fluorescence of abdominal organs were measured.

### Data Analysis

NIR fluorescence data generated with the Mini-FLARE system were analyzed using the Mini-FLARE software package. Regions-of-interest were drawn on the outline of the tumor, liver, kidney, spleen, stomach, small bowel, colon, and bladder as traced manually by visual interpretation on the white light image. Subsequently, fluorescence intensity was automatically calculated and exported to statistical analysis software.

### Fluorescence Microscopy

After intraoperative imaging experiments at 48 or 96 h, the liver was excised completely for *ex vivo* fluorescence measurements. Subsequently, liver tumors were sliced in two to examine internal fluorescent patterns using the Mini-FLARE system. Excised tumor slices were snap-frozen on dry ice and stored at  $-80^{\circ}$ C or were fixed in 10% buffered formalin overnight, washed in 70% ethanol, and subsequently embedded in paraffin. Frozen tissue sections were measured

for fluorescence using the Nuance multispectral imager (CRi, Woburn, MA) mounted on a Leica DM IRE2 inverted microscope (Leica, Wetzlar, Germany), and subsequently stained with hematoxylin and eosin. White light images were created using the same microscope, and subsequently merged with fluorescence images.

### Statistical Analysis

Statistical analysis and generation of graphs were performed using GraphPad Prism Software (ver. 5.01; La Jolla, CA) and SPSS (ver. 17.0; SPSS Inc., Chicago, IL). Fluorescence intensity and tumor size were reported as mean and standard deviation. To test differences between dose groups and time groups, repeated measures ANOVA was used with rat as random factor and dose, time, and dose by time interaction as fixed effects. When the dose by time interaction was not significant, it was subsequently removed from the model. Comparisons between doses and between time points were performed using least square difference (LSD) adjustment for multiple testing. Statistical tests were two-tailed and  $P < 0.05$  was considered significant.

## RESULTS

### Intraoperative Detection of Colorectal Liver Metastases

In 18 rats, syngeneic colorectal liver metastases were induced using the colorectal cancer rat cell line CC531. The mean number of metastases per rat was  $1.8 \pm 0.8$  (range 1–3). The mean size of the liver metastases was  $5.2 \pm 0.3$  mm (range 1.2–13.4 mm). In all 18 rats, all colorectal liver metastases ( $n = 34$ ) were identified using ICG and the Mini-FLARE imaging system (Fig. 1).

### Dose of ICG and Time of Intraoperative Imaging

To determine the influence of ICG dosage and time of imaging, rats were allocated to three dose groups and imaged at four time points and tumor-to-liver ratios (TLRs) were calculated. At all time-points (24, 48, 72, and 96 h) and in all dose groups (0.04, 0.08, and 0.16 mg), fluorescence intensity of liver metastases was significantly higher than the fluorescent intensity of normal liver tissue ( $P < 0.001$ ). Average TLR over all

groups was  $3.0 \pm 1.2$ . The highest average TLR ( $4.3 \pm 1.8$ ) was reached in the 0.08 mg dose group and 72 h after intravenous administration (Fig. 2C).

Repeated measures ANOVA was used to test for differences in TLR between dose and time groups. There was a significant effect of time ( $P < 0.001$ ), but the effects of dose ( $P = 0.12$ ) and dose by time interaction ( $P = 0.91$ ) were not significant. Dose by time interaction was therefore removed from the model. Consequently, the model included rat as random factor and dose and time as fixed effects. This model showed that the TLR was significantly higher in the 72 h time group compared to the 24 h ( $P < 0.001$ ), 48 h ( $P = 0.001$ ), and 96 h ( $P = 0.004$ ) time groups (Fig. 2D). Also, the TLR was significantly higher in the 96 h time group compared to the 24 h group ( $P = 0.049$ ). ICG dose did not significantly influence TLRs, but a trend was found favoring the 0.08 mg dose group (0.08 versus 0.04,  $P = 0.06$ ; 0.08 versus 0.16,  $P = 0.09$ ).

### Biodistribution of Indocyanine Green

Fluorescent intensity of the metastases, liver, kidney, stomach, spleen, small bowel, colon, and bladder was measured at all time points and in all dose groups (data not shown).

Repeated measures ANOVA was used to test for differences in fluorescent intensity of the liver (Fig. 2A) and liver metastases (Fig. 2B) between dose and time groups. Dose by time interaction did not significantly effect liver signal ( $P = 0.1$ ) and metastases signal ( $P = 0.125$ ) and was, therefore, removed from the model. There was a significant effect of time on both liver signal ( $P < 0.001$ ) and liver metastases signal ( $P < 0.001$ ). No significant effect of dose was found on liver signal ( $P = 0.061$ ) and metastases signal ( $P = 0.152$ ). This model showed that liver signal and metastases signal were both significantly higher in the 24 h group compared with all other time-points ( $P < 0.001$ ).

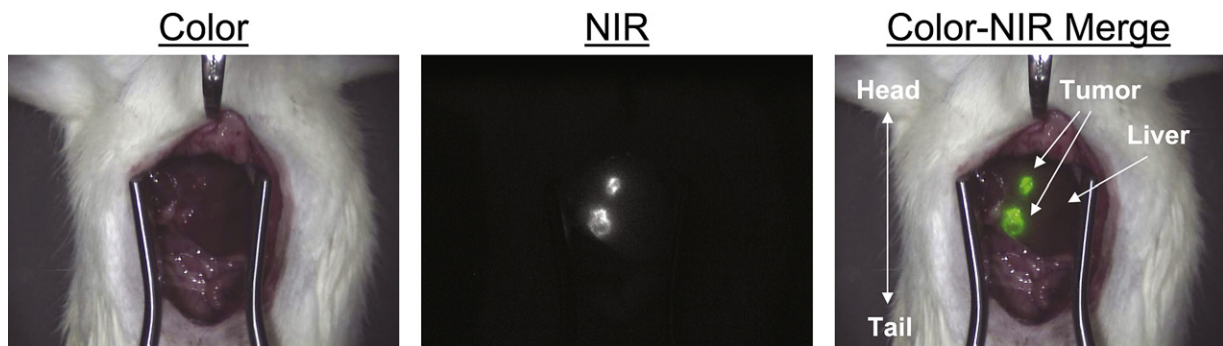


**FIG. 1.** Intraoperative detection of colorectal liver metastases using NIR fluorescence: Shown are a color image (left), a NIR fluorescence image (middle) and a pseudo-colored green merge (right) of two CC531 colorectal liver metastases intraoperatively detected using NIR fluorescence in a male rat 72 h after injection of 0.08 mg indocyanine green. (Color version of figure is available online.)

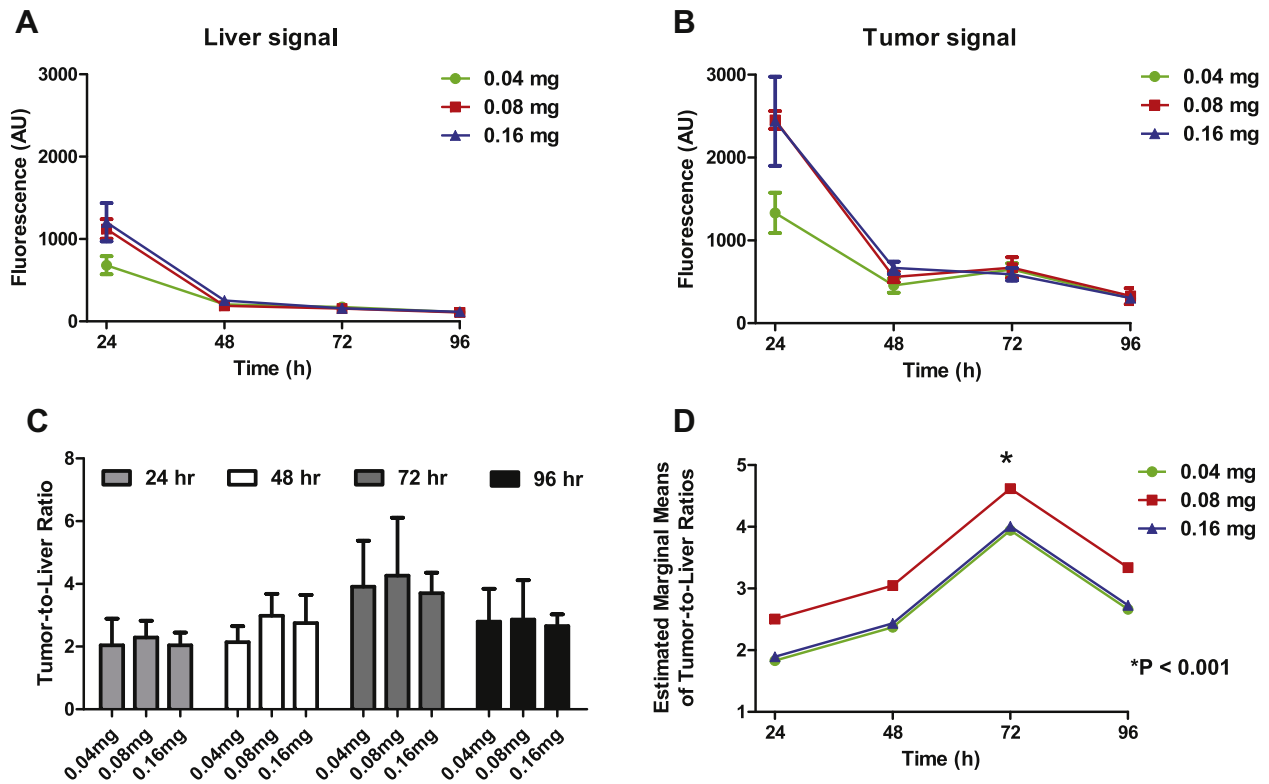


**FIG. 2.** Dose of ICG and timing of intraoperative imaging: (A) Fluorescent intensity of the liver in 18 rats injected with 0.04, 0.08, or 0.16 after 24, 48, 72, and 96 h. (B) Fluorescent intensity of all liver tumors ( $n = 34$ ) in 18 rats injected with 0.04, 0.08, or 0.16 mg ICG after 24, 48, 72, and 96 h. (C) Average tumor-to-liver ratios and standard deviations are plotted for all liver metastases ( $n = 34$ ) in 18 rats injected with 0.04, 0.08, or 0.16 mg ICG after 24, 48, 72, and 96 h. (D). Estimated marginal means of tumor-to-liver ratio for rats injected with 0.04, 0.08, or 0.16 mg ICG after 24, 48, 72, and 96 h using the repeated measures ANOVA and least square difference (LSD) adjustment for multiple testing. This model showed that the tumor-to-liver ratio was significantly higher in the 72 h time group compared to the 24 h ( $P < 0.001$ ), 48 h ( $P = 0.001$ ), and 96 h ( $P = 0.004$ ) time groups. ICG dose did not significantly influence tumor-to-liver ratios, but a trend was found favoring the 0.08 mg dose group (0.08 versus 0.04,  $P = 0.06$ ; 0.08 versus 0.16,  $P = 0.09$ ). (Color version of figure is available online.)

NIR fluorescence intensity of all organs except for the stomach, colon, and the small bowel, was lower or equal to the liver signal. Fluorescence intensity of the stomach, colon, and small bowel was significantly higher compared with other organs and had a maximum at 48 and 72 h.

#### Microscopic Distribution of ICG in Liver Metastases

To determine the precise location of ICG in the vicinity of the tumor, sliced liver metastases were examined for internal fluorescent patterns using the Mini-FLARE system. In all liver metastases, a clear fluorescent rim around the tumor was found. Frozen tissue sections were examined using the Nuance multispectral imager (CRi, Woburn, MA) mounted on a Leica DM IRE2 inverted microscope (Leica, Wetzlar, Germany). A clear fluorescent rim was found in stromal tissue in the transition area between tumor and normal liver tissue in all liver metastases. In this area, multiple cell types that are involved in tissue inflammation (e.g., granulocytes, lymphocytes) were found (Fig 3).

#### DISCUSSION

In the present study, significant differences in TLR were shown between four different time points after ICG administration, with an optimal time of imaging of 72 h after ICG administration. No significant effects were found with regard to dose level; however, a trend was shown favoring 0.08 mg. Moreover, all liver metastases, even as small as 1.2 mm, could be clearly identified during liver surgery using clinically available ICG and the Mini-FLARE system in this syngeneic rat model.

Highest TLRs were reached 72 h after ICG administration. Fluorescence intensity of the liver and the liver metastases were also examined separately. Fluorescent intensity of the liver decreased strongly after 24 h and was not dose-dependent. Fluorescent intensity of the liver metastases also decreased strongly at 48 h, but a small, nonsignificant peak was found at 72 h. This small peak can be explained by the re-uptake of ICG in the small bowel as part of the enterohepatic circulation and subsequent passage through the bowel tract, hence the highest TLR at 72 h.



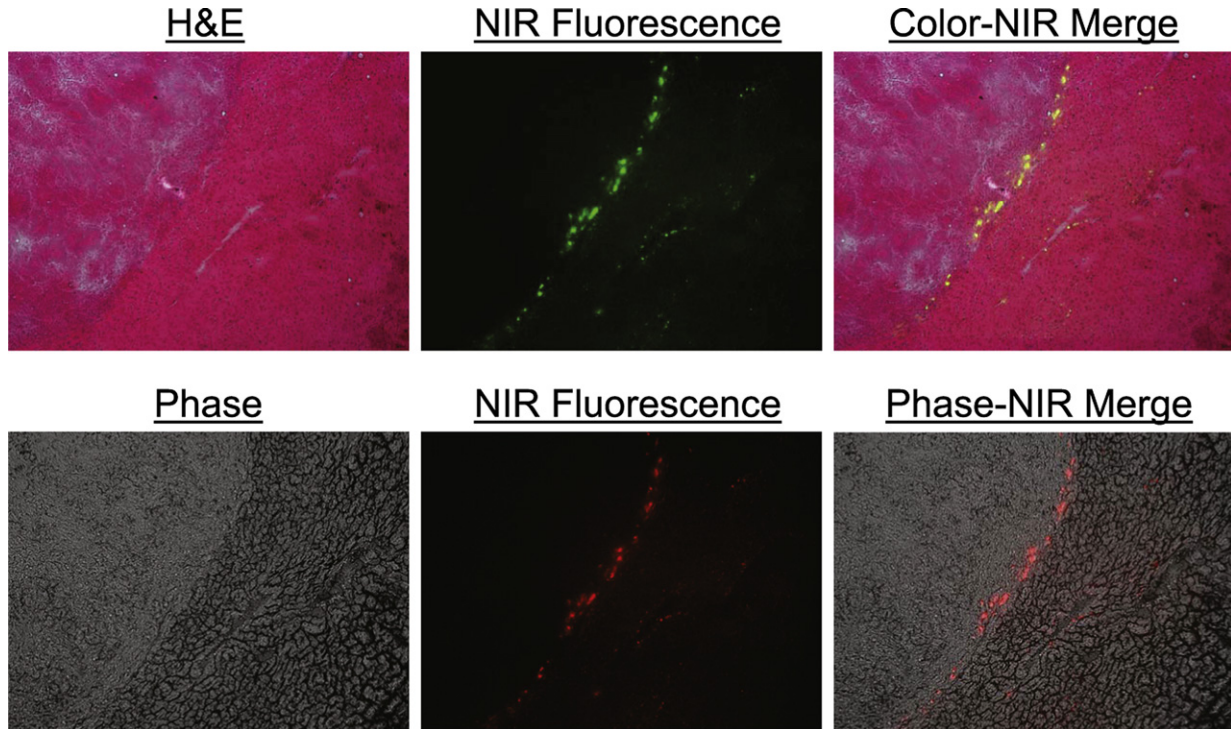


**FIG. 3.** Fluorescent microscopy of a colorectal liver metastasis: Shown are a hematoxylin and eosin staining (top left), a pseudo-colored green NIR fluorescence image (top middle), and pseudo-colored green merge (top right) of a 20  $\mu\text{m}$  frozen tissue section of a colorectal liver metastasis. Furthermore, a phase image (bottom left), a pseudo-colored red NIR fluorescence image (bottom middle), and a pseudo-colored red merge (bottom right) of a 20  $\mu\text{m}$  frozen tissue section of a colorectal liver metastasis is shown. The fluorescent rim in stromal tissue in the transition area between tumor and normal liver tissue can be clearly identified. (Color version of figure is available online.)

Regarding ICG dosage, a trend was found favoring the 0.08 mg ICG group. Extrapolating to human body weight, this dose corresponds to a dose of 20 mg ICG, which is frequently used in a clinical setting. To optimize this technique in clinical practice, a dose-finding study is imperative. As ICG is already clinically available and FDA-approved, a straightforward translation of our results to the clinic can be made.

It is known that a substantial part of liver metastases, mainly the small (<5 mm) and superficially located, cannot be identified using conventional imaging modalities such as CT or IOUS. Size of metastases in the present study varied from 1.2 to 13.4 mm of which 50% were smaller than 5 mm. This emphasizes that ICG fluorescence in liver surgery might be of great value in detecting small colorectal liver metastases. As the currently used preclinical animal model only generated colorectal liver metastases, future clinical studies will have to determine the ability of this technique to discriminate between malignant and benign lesions of the liver.

Since maximum penetration depth of NIR fluorescence is currently up to 1 cm, identification of non-superficially situated liver metastases will be more challenging. Therefore, intraoperative ICG fluorescence must be regarded as a complement on currently used conventional imaging modalities such as IOUS

and CT. Improvements in imaging systems, NIR fluorescence contrast agents, and software and reduction in background fluorescence may facilitate NIR fluorescence imaging of deeper located metastases.

The currently used technique to detect liver metastases using NIR fluorescence and ICG is based on the clearance capacity of the liver. It has been described that in patients with a cirrhotic liver, or in patients pre-treated with chemotherapy, the liver function and clearing capacity can be reduced. A reduced liver function could also affect the clearance of ICG, which can result in a higher background signal and, therefore, lower contrast. However, it has been shown that even cirrhotic livers have an extensive clearance capacity [16]. This implies that the currently used technique can probably be used in subjects with a reduced liver function, although, in these patients, the optimal time interval between ICG administration and imaging could be longer. Future clinical studies have to elaborate on this topic.

A recent development in liver surgery is the introduction of laparoscopic surgery. NIR fluorescence can be of great value, also in laparoscopic surgery, since palpation of the liver is not possible and the surgeon can only rely on visual inspection and preoperative imaging. To anticipate this potential new application,

laparoscopic NIR fluorescence camera systems are presently being developed and tested [17, 18].

In summary, this study demonstrates clear identification of colorectal liver metastases during surgery using the clinically available NIR fluorescent agent ICG and the Mini-FLARE system. Imaging 72 h after administration of 0.08 mg ICG provided the highest TLRs. In particular, the ability to detect small (<5 mm) and superficially located metastases can be of great value during liver surgery. When the current intraoperative identification of colorectal liver metastases can be improved using this technique, the resection can potentially be performed more accurately, and preoperatively missed metastases can be involved in surgical decision making.

#### ACKNOWLEDGMENTS

This study was performed within the framework of CTMM, the Center for Translational Molecular Medicine (DeCoDe project, grant 030-101). This study was supported by the Sacha Swartttouw-Hijmans Foundation and National Institutes of Health grants R01-CA-115296 and R01-EB-010022.

#### REFERENCES

1. Parkin DM, Bray F, Ferlay J, et al. Global cancer statistics, 2002. *CA Cancer J Clin* 2005;55:74.
2. Manfredi S, Lepage C, Hatem C, et al. Epidemiology and management of liver metastases from colorectal cancer. *Ann Surg* 2006;244:254.
3. Ruers T, Bleichrodt RP. Treatment of liver metastases, an update on the possibilities and results. *Eur J Cancer* 2002;38:1023.
4. Simmonds PC, Primrose JN, Colquitt JL, et al. Surgical resection of hepatic metastases from colorectal cancer: A systematic review of published studies. *Br J Cancer* 2006;94:982.
5. Wei AC, Greig PD, Grant D, et al. Survival after hepatic resection for colorectal metastases: A 10-year experience. *Ann Surg Oncol* 2006;13:668.
6. Pawlik TM, Scoggins CR, Zorzi D, et al. Effect of surgical margin status on survival and site of recurrence after hepatic resection for colorectal metastases. *Ann Surg* 2005;241:715. discussion.
7. Abdalla EK, Vauthey JN, Ellis LM, et al. Recurrence and outcomes following hepatic resection, radiofrequency ablation, and combined resection/ablation for colorectal liver metastases. *Ann Surg* 2004;239:818.
8. Karanjia ND, Lordan JT, Fawcett WJ, et al. Survival and recurrence after neo-adjuvant chemotherapy and liver resection for colorectal metastases: A ten year study. *Eur J Surg Oncol* 2009;35:838.
9. Leen E, Ceccotti P, Moug SJ, et al. Potential value of contrast-enhanced intraoperative ultrasonography during partial hepatectomy for metastases: An essential investigation before resection? *Ann Surg* 2006;243:236.
10. Sahani DV, Kalva SP, Tanabe KK, et al. Intraoperative US in patients undergoing surgery for liver neoplasms: Comparison with MR imaging. *Radiology* 2004;232:810.
11. Nomura K, Kadoya M, Ueda K, et al. Detection of hepatic metastases from colorectal carcinoma: Comparison of histopathologic features of anatomically resected liver with results of preoperative imaging. *J Clin Gastroenterol* 2007;41:789.
12. Ishizawa T, Fukushima N, Shibahara J, et al. Real-time identification of liver cancers by using indocyanine green fluorescent imaging. *Cancer* 2009;115:2491.
13. Vahrmeijer AL, van Dierendonck JH, Schutrups J, et al. Potentiation of the cytostatic effect of melphalan on colorectal cancer hepatic metastases by infusion of buthionine sulfoximine (BSO) in the rat: Enhanced tumor glutathione depletion by infusion of BSO in the hepatic artery. *Cancer Chemother Pharmacol* 1999;44:111.
14. Mieog JS, Troyan SL, Hutteman M, et al. Towards optimization of imaging system and lymphatic tracer for near-infrared fluorescent sentinel lymph node mapping in breast cancer. *Ann Surg Oncol* 2011, in press.
15. Troyan SL, Kianzad V, Gibbs-Strauss SL, et al. The FLARE intraoperative near-infrared fluorescence imaging system: A first-in-human clinical trial in breast cancer sentinel lymph node mapping. *Ann Surg Oncol* 2009;16:2943.
16. Bloemen JG, Olde Damink SW, Venema K, et al. Short chain fatty acids exchange: Is the cirrhotic, dysfunctional liver still able to clear them? *Clin Nutr* 2010;29:365.
17. Matsui A, Tanaka E, Choi HS, et al. Real-time intra-operative near-infrared fluorescence identification of the extrahepatic bile ducts using clinically available contrast agents. *Surgery* 2010;148:87.
18. van der Pas MH, van Dongen GA, Cailier F, et al. Sentinel node procedure of the sigmoid using indocyanine green: Feasibility study in a goat model. *Surg Endosc* 2010;24:2182.